RESEARCH

Effect of Heating on Protein Denaturation, Water State, Microstructure, and Textural Properties of Antarctic Krill (*Euphausia superba*) Meat

Peizi Sun[1] · Junxin Lin[1] · Xiang Ren[1] · Biao Zhang[1] · Jiaxin Liu[1] · Yanfen Zhao[1] · Dongmei Li[1,2,3]

Abstract

Antarctic krill (*Euphausia superba*) is an important source of biomass and high-quality protein. However, heat treatment negatively impacts the quality of Antarctic krill and compromises its utilization in the food industry. This study aimed to investigate the mechanisms underlying changes in Antarctic krill meat characteristics and physicochemical properties treated at different temperatures and holding times. Our findings indicated that hardness and cooking loss of Antarctic krill meat increased dramatically at higher temperatures and holding times. The low-field nuclear magnetic resonance (LF-NMR) analysis revealed that the loss of immobilized water increased, whereas the SDS-PAGE analysis showed that the content of myosin heavy chain decreased significantly and that protein degradation occurred. Fourier transform infrared spectroscopy (FT-IR) and intrinsic fluorescence spectra suggested that α-helix motifs were transformed into β-sheets and that more hydrophobic groups were exposed. The scanning electron microscopy (SEM) results showed that Antarctic krill meat formed corrugated folded regions after heat treatment without forming a three-dimensional water-entrapped structure, which led to significant water loss, resulting in rapid deterioration of Antarctic krill meat. These results provide the basis for a deeper understanding of the processing characteristics of Antarctic krill meat.

Keywords Antarctic krill (*Euphausia superba*) · Heat treatment · Texture · Myofibrillar proteins · Water distribution

Introduction

Antarctic krill (*Euphausia superba*), a crustacean zooplankton, is considered one of the largest and last biological resources on earth (approximately 379 million tons) (Atkinson et al., 2009). It has become the focus of fishing powers because of the increasing tension in fishery resources. Antarctic krill is rich in protein, and its water, crude protein, total fat, and chitin contents are 77.9–83.1%, 11.9–15.4%, 0.4–3.6%, and 2%, respectively (Cavan et al., 2019). In addition, krill protein is rich in essential amino acids necessary for humans, and the biological value of krill protein is higher than those of milk or other animal proteins (Peng et al., 2019). The main products derived from fishing and processing of Antarctic krill include frozen krill, krill meal, krill oil, dried krill, and shelled krill meat; however, only Antarctic krill oil has become a profitable product (Liu et al., 2011). Thus, the protein resource in Antarctic krill remains largely underutilized (Wang et al., 2015), which can be linked to its unique processing method (Chen & Jaczynski, 2007). The quality of its meat rapidly deteriorates after heat treatment, increasing its hardness and generally resulting in poor sensory acceptance compared to white shrimp and/or shrimp products (Lin et al., 2021). However, the reasons underlying these changes in Antarctic krill protein during heat treatment are poorly known.

Heat treatment is an important step in meat and seafood processing (Wang et al., 2013). Heat treatment imparts particular features such as color, flavor, and texture to foods, as well as contributes to protein denaturation, thus enhancing protein digestibility and absorption. In addition, heat treatment is mostly bactericidal, which improves food safety (Hassoun et al., 2021). However, excessive heat treatment can cause quality loss (Urango et al., 2022), especially

✉ Dongmei Li
426417898@qq.com

1   School of Food Science and Technology, National Engineering Research Center of Seafood, Dalian Polytechnic University, Dalian 116034, Liaoning, China

2   Engineering Research Center of Seafood of Ministry of Education of China, Dalian 116034, Liaoning, China

3   Collaborative Innovation Center of Seafood Deep Processing, Dalian Polytechnic University, Dalian 116034, Liaoning, China

related to texture, including hardness, chewiness, and cohesiveness, which results in coarser texture, reduced sensory acceptability, and even loss in edible value (Zhang et al., 2016).

The changes in texture are related to water-holding capacity, which usually affects the tenderness, tissue structure, and sensory quality of meat (Bi et al., 2019). (Chen et al., 2022) demonstrated that increasing the water-holding ratio increased meat tenderness. Conversely, texture changes are mainly linked to protein denaturation induced by heat treatment, which leads to protein aggregation and coagulation and contraction of myofibrillar proteins, resulting in harder meat and more compact tissue texture (Ling et al., 2015). Meat proteins are usually constituted by myofibrillar proteins; thus, changes in myofibrillar proteins directly impact meat quality (Huang et al., 2016). The autolysis in Antarctic krill protein degrades it into a more water-soluble protein. The Antarctic krill has a higher water-soluble protein content and lower salt-soluble myofibrillar proteins (approximately 20%). Conversely, its myofibrillar protein content differs significantly from those of other aquatic products (approximately 75%) (Ellingsen & Mohr, 1987). Nonetheless, no reports are available on how Antarctic krill myofibrillar proteins change and how these changes affect the microstructure and macrotexture quality.

This study aims to explore the effect of heat treatment at different temperatures and holding times on Antarctic krill meat texture. In addition, we have investigated the relationship between the texture of Antarctic krill meat and changes in water state, tissue microstructure, and protein structure. This study provides a theoretical basis for further exploration of protein resources of Antarctic krill.

Materials and Methods

Materials and Chemicals

Frozen Antarctic krill (*Euphausia superba*) was supplied by Dalian Liaoyu Fishery Group Co. (Dalian, China). Coomassie Brilliant Blue R-250, KBr, sodium dodecyl sulfate (SDS), protein molecular weight marker, and bovine serum albumin (BSA) were purchased from Solarbio Co., Ltd. (Beijing, China). The bicinchoninic acid (BCA) assay kit was purchased from Nanjing Jiancheng Co., Ltd. (Nanjing, China). All chemicals used in this study were of analytical grade and required no further purification.

Heat Treatment

Frozen Antarctic krill meat (individual krill meat intact and relatively uniform in size) was placed in a self-sealing bag and thawed at 4 °C in a refrigerator for 24 h. After thawing, the krill meat was rinsed in a container until individual krill meat was evenly dispersed in the water and free of impurities. They were then transferred to a stainless-steel sieve, evenly distributed, and left to dry for 10 min. The krill meat with no visible moisture on the surface was weighed and loaded into separate centrifuge tubes. Subsequently, 5.00 ± 0.02 g of krill meat was placed in each centrifuge tube. The samples were placed in batches in preheated water baths at 55, 65, 75, 85, and 95 °C for 2, 4, 6, 8, and 10 min. The cooking loss and texture profile analyses for all samples, and other indices for samples A, B, C, D, E, F, G, H, I, J were analyzed which corresponded to: A, untreated sample; B, 55 °C /10 min; C, 65 °C /10 min; D, 75 °C /10 min; E, 85 °C /10 min; F, 95 °C /2 min; G, 95 °C /4 min; H, 95 °C /6 min; I, 95 °C /8 min; and J, 95 °C /10 min. After heat treatment, samples were immediately left to cool in ice water. The unheated krill meat was used as the negative control. The heat-treated samples were stored in ice before further analyses.

Extraction of Myofibrillar Proteins

The extraction of myofibrillar proteins was performed according to (Yang et al., 2019), and all experiments were performed at 4 °C. The treated samples were mixed with four times the volume of phosphate buffer (50 mM sodium phosphate buffer, pH 7.0) using a homogenizer (T-25, IKA, Guangzhou, China) at 10,000 rpm on ice and subjected to six cycles of homogenization for 30 s in duplicate. A rest interval of 30 s was provided to prevent overheating before the start of next round. The obtained homogenized solution was centrifuged at $8,000 \times g$ for 15 min at 4 °C. The precipitate was collected and further homogenized with four times the volume of phosphate buffer (0.6 M NaCl, 50 mM sodium phosphate buffer, pH 7.0). Homogenization was repeated using the procedure described above, and the homogenized solution was left overnight at 4 °C. After sufficient sedimentation, the homogenized solution was centrifuged at $8,000 \times g$ for 15 min at 4 °C. The supernatant was collected and considered myofibrillar protein solution, which was then stored at 4 °C for subsequent experiments. The content of myofibrillar protein in the supernatant was determined using the BCA kit with BSA as the protein standard.

Texture Profile Analysis (TPA)

The TPA was carried out according to the method described by (Chen et al., 2020) with some modifications. The TPA of samples heated at different temperatures and holding times was performed using a texture analyzer equipped with a cylindrical probe P50 (TA.XTplus, Stable Micro Systems Ltd., Godalming, UK). The pre-test, test, and post-test

speeds were 1.00, 2.00, and 15.00 mm/s, respectively. The deformation rate adopted in the analysis was 50%. The texture analysis of each sample was performed in triplicate.

Cooking Loss Analysis

The cooking loss was calculated by dividing the difference in the krill meat weight before and after heating by the weight of raw krill meat, and the result was expressed as a percentage (Eq. 1) according to the method proposed by (Lee et al., 2021):

$$\text{Cooking loss } (\%) = \left(M_0 - M_1\right)/M_0 \times 100 \tag{1}$$

where M_0 is the weight of raw krill meat, and M_1 is the weight of krill meat after heat treatment.

Low-Field Nuclear Magnetic Resonance (LF-NMR)

The transverse relaxation times (T_2) of heated Antarctic krill meat were measured using an LF-NMR analyzer (MesoMR23-060 V-I, Suzhou Niumag Corporation, Suzhou, China) using the method proposed by (Chen et al., 2015) with slight modifications. The heat-treated krill meat (1 g) was weighed, covered with a plastic wrap, and placed in a 60-mm-diameter chamber. The decay signals were collected with a Carr-Purcell-Meiboom-Gill (CPMG) sequence using a magnetic field strength of 0.5 T and the temperature of operation of permanent magnets at 32 °C. The T_2 measurements were performed using the following parameters: τ value, 200 μs (time between 90 and 180 pulses) with two pulse lengths of 21.0 and 42.0 μs; number of echoes (NECH), 4500; number of scans, 8. The distributed multi-exponential fits of CPMG decay curves were performed using the MultiExp Inv analysis software (Suzhou Niumag Analytical Instrument Co., Suzhou, China) via the simultaneous iterative reconstruction technique (SIRT).

Magnetic Resonance Imaging (MRI)

The MRI analysis was performed according to (Xu et al., 2020) with some modifications. Briefly, 3 g of krill samples were accurately weighed and placed in a round plastic box. The proton density images were acquired using a multi-spin echo (MSE) sequence. The MRI data were acquired using a 0.5 T permanent magnet (MesoMR23-060 V-I, Suzhou Niumag Corporation, Suzhou, China) equipped with a 30 mm radiofrequency coil at 32 °C. The measurements were performed under the following conditions: field of view (FOV), 100 mm × 100 mm; slice width, 2.3 mm; read size, 256; phase size, 192; TE and TR arguments, 20 and 2000 ms, respectively. The images were pseudo-colored and

quantified using OsiriX software (OsiriX Lite version 7.0.4, Geneva, Switzerland).

Scanning Electron Microscopy (SEM)

Prior to SEM analysis, raw and heated krill samples were freeze-dried for 24 h (Li et al., 2021a). Before measurements, the cross sections of krill samples were mounted on short bronze platforms, coated with gold, and analyzed using a scanning electron microscope (JSM-7800F; JEOL, Tokyo, Japan) at 10 kV to determine the micromorphology of heated samples. The micrographs were taken from different points of a single sample with similar magnification rates and width measurements.

Fluorescence Spectroscopy

Emission fluorescence spectroscopy was performed according to the procedure described by (Zhang et al., 2020). Prior to fluorescence analysis, the myofibrillar proteins were diluted to 0.5 mg/mL with 0.6 mol/L NaCl buffer (pH 7.0). The fluorescence spectra of diluted myofibrillar protein solutions were recorded using a spectrophotometer (F-2700, Hitachi Co., Tokyo, Japan) with an excitation wavelength of 280 nm and excitation and emission slit widths of 5 nm. The emission spectra were measured within the 300–450 nm range with a scan rate of 5 nm/s. The solvent emission spectra were recorded under the same conditions to eliminate interference.

Fourier Transform Infrared Spectroscopy (FT-IR)

FT-IR spectroscopy was performed using an FT-IR spectrometer (Perkin Elmer, Salem, MA, USA) following the method proposed by (Zheng et al., 2020). The previously prepared myofibrillar protein solutions were initially frozen at −40 °C for over 4 h and then freeze-dried for 72 h. Next, 1 mg of the sample was mixed with 100 mg of KBr, gently ground into a homogeneous powder, and pressed into transparent tablets under an infrared lamp using an agate mortar and pestle. In transmittance mode, all spectra were acquired within the wavelength range of 4000–400 cm^{-1} with 32 scans and a resolution of 4 cm^{-1} at room temperature. The amide I bands were fitted to a Gaussian curve using Omnic 9.2 software (Nicolet, Madison, WI, USA).

Sodium Dodecyl Sulfate–Polyacrylamide Gel Electrophoresis (SDS-PAGE)

The concentration of myofibrillar proteins in samples was measured using a BCA protein kit. Each sample was diluted to 1.5 mg/mL with the extraction buffer, mixed at a ratio of 1:1 (v/v) with sample loading buffer (0.25 M Tris–HCl, pH

7.4, 8 M urea, 5% SDS, 5% mercaptoethanol), and boiled for 5 min. Next, 10 μL of samples were loaded onto 4% stacking gels and 12% separation gels and labeled with multiple molecular weight markers (20–245 kDa). Electrophoresis was then performed using a mini-stand electrophoresis apparatus (Bio-Rad, USA) with running buffer added at 120 V and 20 mA for 2 h. After electrophoresis, the gels were destained with 50% methanol and 10% acetic acid for 2–3 h until the gel background was clear. After separation and staining, the bands were recorded using Gel Capture software (DNR Bio-Imaging Systems, Jerusalem, Israel) (Ishamri et al., 2019).

Statistical Analysis

All experiments were performed at least three times. Data are presented as the mean $\pm$ standard deviation (SD). The statistical analysis was performed using SPSS version 25 (SPSS Inc., Chicago, IL, USA). ANOVA was used to determine mean value of each parameter, and Duncan's test was applied to determine significant differences ($P < 0.05$) among various conditions. All graphs were created using Origin 2021 pro software (OriginLab Inc., Northampton, MA, USA).

Results and Discussion

TPA Analysis

Texture is an important quality attribute of meat. The changes in texture during heat treatment are directly associated with tissue state, sensory quality, and physical structure

of obtained meat products (Wang et al., 2020). Figure 1 shows changes in hardness (Fig. 1a) and chewiness (Fig. 1b) of Antarctic krill meat treated at different temperatures and holding times. Hardness is the force necessary to attain a given deformation, which is equal to the peak pressure of the sample when it is first pressed. Chewiness is the energy required to masticate food to a state ready for swallowing, which is equal to the product of hardness, cohesiveness, and springiness (Szczesniak, 2002). Both hardness and chewiness increased at higher holding times and temperatures; the higher the temperature, the shorter the time required to reach the equilibrium value. A more significant increase in hardness and chewiness was observed in samples heated at 95 °C for 10 min compared to 95 °C for 8 min.

Heat treatment is often accompanied by denaturation and coagulation of myofibrillar proteins, contraction and exposure of hydrophobic regions of the myofibrillar structure, and significant loss of water between myofibrils, which leads to an increase in hardness of krill meat (Straadt et al., 2007). Interestingly, krill meat samples heated at 85 °C for 10 min exhibited higher hardness and chewiness values than those treated at 95 °C for 10 min. This could be linked to protein degradation induced by heating (Strzelczak et al., 2021), causing severe tissue damage when treated at 95 °C for 10 min. This high temperature might have contributed to further breaking and relaxation of the myofibrillar fibers, leading to a decrease in hardness and chewiness, which is consistent with the results of (Jiang et al., 2018). In addition, the chewiness of krill meat treated at 55 °C for 4 min was higher than those of samples treated at 65 °C for 4 min. Thus, moderate protein denaturation might have occurred in samples treated at 65 °C for 4 min, which led to changes in texture.
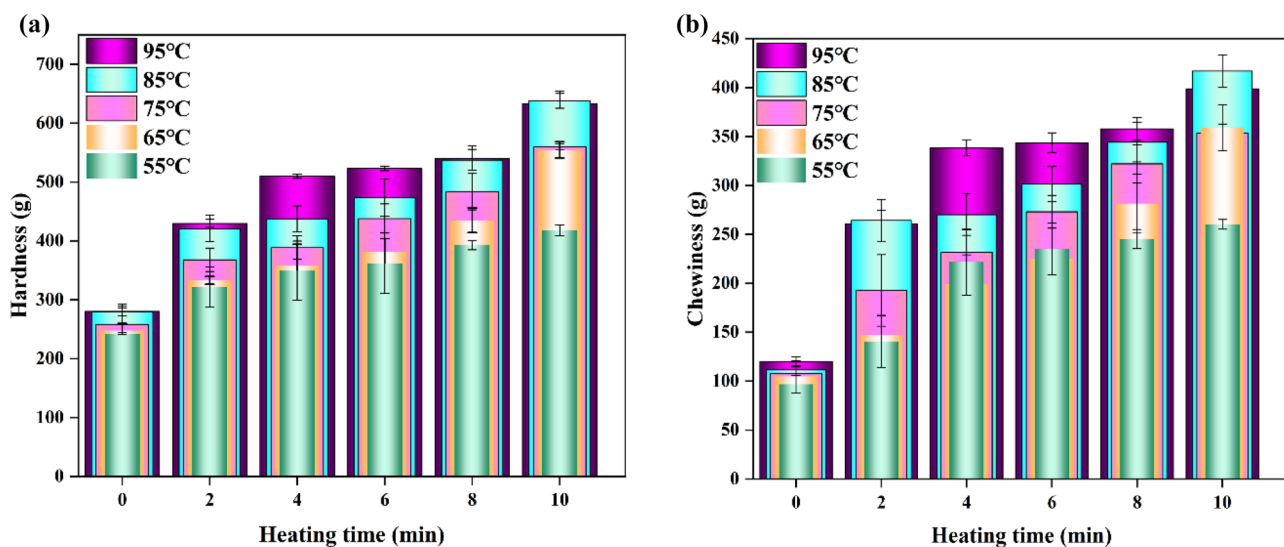

Fig. 1 Texture analysis of Antarctic krill meat subjected to different heat treatments. **a** Hardness. **b** Chewiness

Cooking Loss

Cooking loss is an important factor in heat-treated meat and includes water loss and leakage of lipids, peptides, and other nutrients, resulting in decreased quality (Purslow et al., 2016). The cooking loss rates of krill meat heated at different temperatures and holding times are shown in Fig. 2. The cooking loss of krill meat showed an upward trend with increasing holding times, in which values initially increased and then decreased. Considering the same holding time, higher cooking loss rates were observed at higher temperatures, which could be due to the fact that proteins on the surface of krill meat undergo rapid denaturation, and the muscle tissue rapidly contracts, thus resulting in rapid juice loss (Li et al., 2018). In addition, the cooking loss of krill meat peaked in samples treated at 95 °C for 8 min (up to 43%), while cooking loss in samples treated at 95 °C for 10 min was lower than those of samples treated at 95 °C for 8 min, which was likely due to the almost complete denaturation of proteins after prolonged heating. Moreover, the reduced degree of conversion of water molecules between immobilized and free states might have amplified aggregation of

denatured proteins found on the surface of krill meat with myofibrils, preventing water transfer and decelerated cooking loss (Haghighi et al., 2021). (Niamnuy et al., 2008) showed that cooking loss rates of white shrimp treated in boiling water at 100 °C for 7 min were within the range of 8–21%, which were significantly lower than those of krill meat found in the present study. This might be related to the lower myofibrillar protein content of Antarctic krill meat.

Proton Dynamics Using LF-NMR

Moisture content and water state are attributes that are closely related to meat texture. Proton spin–spin relaxation times (T_2) can explain the mobility and degrees of freedom of water molecules, thus reflecting dynamic properties of water such as diffusion and state (Zhu et al., 2021). LF-NMR is a commonly used technique to characterize hydrogen protons in different matrices.

The effect of heat treatment on hydrogen proton peaks and relative individual water content of krill meat is shown in Fig. 3 and Tables 1 and 2. Three hydrogen proton peaks were observed in the untreated (sample A) and heat-treated

Fig. 2 Cooking loss of Antarctic krill meat subjected to different heat treatments
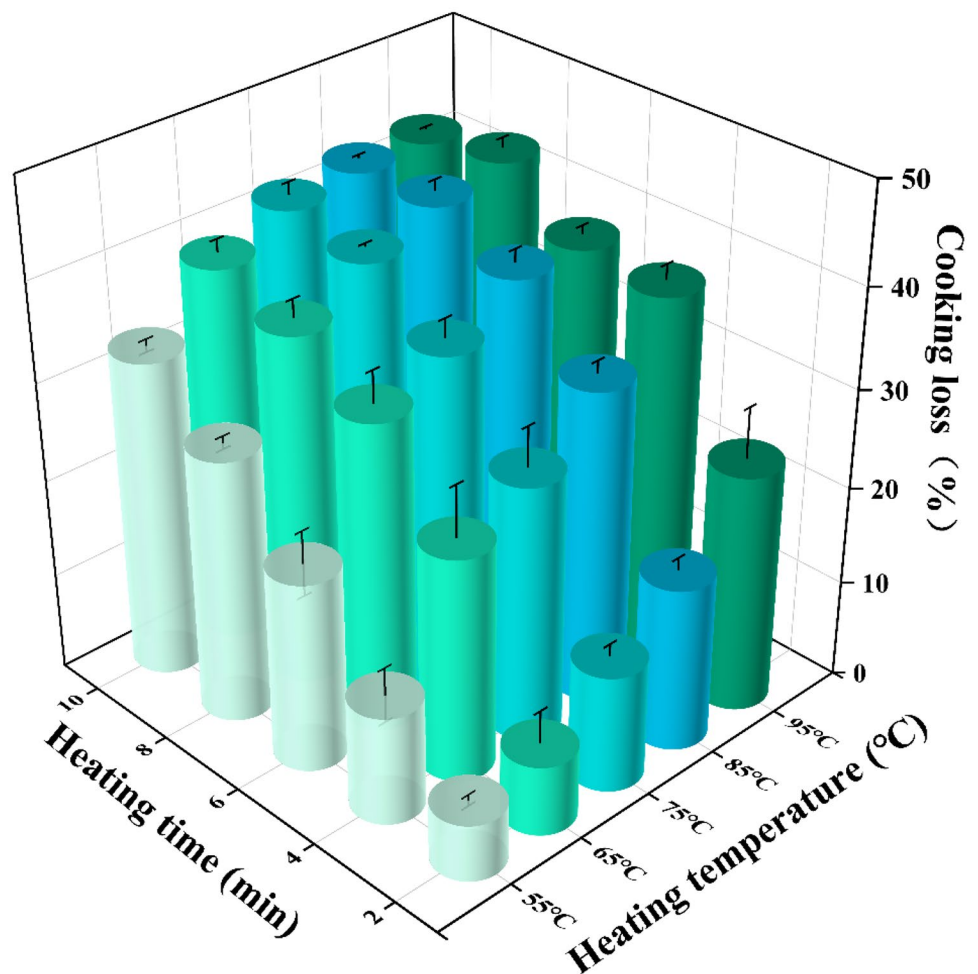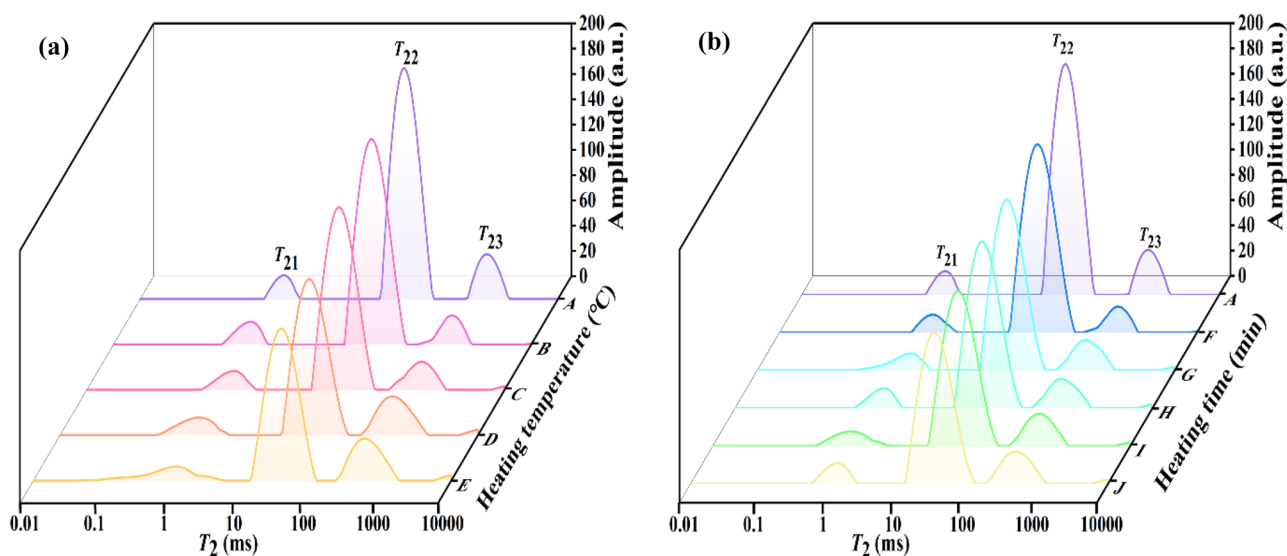
Fig. 3 Water distribution in Antarctic krill meat subjected to different heat treatments. **a** Distribution curves of T_2 relaxation time of samples treated at different temperatures. **b** Distribution curves of T_2 relaxation time of heat-treated samples subjected to different holding times.

A: untreated; B: 55 °C/10 min; C: 65 °C/10 min; D: 75 °C/10 min; E: 85 °C/10 min; F: 95 °C/2 min; G: 95 °C/4 min; H: 95 °C/6 min; I: 95 °C/8 min; J: 95 °C/10 min

krill meat samples: T_{21} peak (0–10 ms) indicated water associated with macromolecules, i.e., bound water; T_{22} peak (10–100 ms) indicated immobilized water located between fine and thick filaments of the myofibrillar protein network; T_{23} peak (100–1000 ms) was attributed to free water in myofibril lattice (Ling et al., 2020). Changes in T_{21} peak values did not significantly differ for heated krill samples compared with untreated samples, which could be explained by the stable degree of binding of water to macromolecules of myofibrils during heat treatment. In contrast to untreated krill meat (sample A), T_{22} and T_{23} relaxation times of all heat-treated samples gradually decreased at higher temperatures and longer holding times.

Figure 3a and Table 1 show T_2 relaxation times and peak regions of krill meat at different heating temperatures. Compared with sample A, T_{22} and T_{23} of samples B, C, D, and E decreased gradually with an increase in temperature. T_{22} and T_{23} decreased to 27.36 ms and 440.47 ms in sample

A and 12.75 ms and 186.89 ms in group E, respectively. The heated krill meat samples undergo protein denaturation and muscle contraction, which affects the degrees of freedom of water molecules by restraining them and reducing their mobility, leading to peak blueshift; these observations are consistent with those of (Sun et al., 2020). In contrast to the untreated sample (sample A), T_{22} of samples F, G, H, I, and J decreased significantly with prolonged holding times; hence, immobilized water was more affected. In addition, T_{23} of samples G, H, I, and J did not change significantly, which could be due to the fact that the degrees of freedom of water molecules had reached equilibrium in samples treated at 95 °C for 4 min and did not change significantly with prolonged heating (Fig. 3b and Table 2).

A_{21}, A_{22}, and A_{23} represent peak areas of bound water, immobilized water, and free water in krill meat, respectively, representing the relative water content (Tables 1 and 2). A_{21} peak areas of samples A, B, C, D, E, and F, G, H, I, J changed

Table 1 T_2 relaxation times and peak areas of Antarctic krill muscle after treatment at different temperatures

Sample	Heat treatment	T_{21} (ms)	T_{22} (ms)	T_{23} (ms)	A_{21} (g^{-1})	A_{22} (g^{-1})	A_{23} (g^{-1})
A	Untreated	0.26±0.04[a]	27.36±0.00[a]	401.09±15.89[a]	233.89±10.25[a]	2799.46±41.66[a]	442.42±3.51[d]
B	55 °C/10 min	0.26±0.22[a]	20.27±0.80[b]	230.17±9.12[b]	297.18±63.24[a]	2680.82±16.56[b]	405.43±8.81[e]
C	65 °C/10 min	0.27±0.22[a]	16.08±0.65[c]	214.73±8.51[bc]	243.90±33.76[a]	2555.46±14.92[c]	456.02±0.61[c]
D	75 °C/10 min	0.15±0.12[a]	14.32±0.57[d]	200.33±7.93[cd]	292.32±50.66[a]	2246.01±11.23[d]	597.77±6.71[b]
E	85 °C/10 min	0.33±0.37[a]	12.75±0.53[e]	186.89±7.40[d]	294.25±8.62[a]	2187.11±8.99[e]	620.92±4.19[a]

A: untreated sample; B: 55 °C/10 min; C: 65 °C/10 min; D: 75 °C/10 min; E: 85 °C/10 min. Data are presented as means±SD (n=3). Different lowercase letters (a, b, c, d, e) indicate significant differences in transverse relaxation time and water proportion ($P < 0.05$) between treatments at different temperatures

Table 2 T_2 relaxation times and peak areas of Antarctic krill muscle after treatment at different holding times

Sample	Heat treatment	T_{21} (ms)	T_{22} (ms)	T_{23} (ms)	A_{21} (g^{-1})	A_{22} (g^{-1})	A_{23} (g^{-1})
A	Untreated	0.26 ± 0.04^a	27.36 ± 0.00^a	401.09 ± 15.89^a	233.89 ± 10.25^a	2799.46 ± 41.66^a	442.42 ± 3.51^b
F	95 °C/2 min	0.55 ± 0.17^a	19.80 ± 0.80^b	224.90 ± 9.12^b	207.47 ± 25.98^a	2703.54 ± 26.64^b	271.50 ± 6.97^e
G	95 °C/4 min	0.26 ± 0.10^a	15.00 ± 0.61^c	187.20 ± 15.34^c	246.34 ± 32.10^a	2425.71 ± 15.20^c	414.32 ± 3.30^c
H	95 °C/6 min	0.35 ± 0.30^a	13.36 ± 0.53^d	174.36 ± 6.91^c	254.52 ± 57.62^a	2408.15 ± 10.38^c	434.31 ± 4.51^b
I	95 °C/8 min	0.33 ± 0.17^a	11.90 ± 0.00^e	166.65 ± 11.56^{cd}	222.74 ± 25.88^a	2314.86 ± 6.90^d	369.03 ± 5.59^d
J	95 °C/10 min	0.42 ± 0.09^a	11.36 ± 0.46^e	151.75 ± 6.01^d	258.95 ± 34.57^a	2303.79 ± 12.35^d	459.02 ± 7.00^a

A: untreated; G: 95 °C/4 min; F: 95 °C/2 min; H: 95 °C/6 min; I: 95 °C/8 min; J: 95 °C/10 min. Data are presented as means $\pm$ SD (n = 3). Different lowercase letters (a, b, c, d, e) indicate significant differences in transverse relaxation time and water proportion ($P < 0.05$) between treatments at different holding times

only slightly in heated samples, indicating that heating did not significantly change the content of bound water in krill meat. Compared with untreated sample A, A_{22} peak areas of samples B, C, D, and E decreased significantly at higher temperatures, thus indicating a possible decrease in the content of immobilized water between fibers induced by heating. This could cause myofibrils to contract and disrupt protein structure, resulting in water release from within the myofibril into the inter-myofibrillar space and, consequently, in water loss (Xia et al., 2018). The A_{22} peak area in samples F, G, H, I, and J decreased with prolonged heating time. Overall, the A_{23} peak area in samples B, C, D, E, and F, G, H, I, J showed an upward trend, indicating that protein was progressively degraded and denatured at increasing temperatures and holding times, resulting in gradual conversion of immobilized water into free water. Moreover, the A_{23} peak areas of samples treated at 95 °C for 8 min were lower than those of samples treated at 95 °C for 10 min. This may be linked to severe muscle damage caused by heating at 95 °C for 8 min, resulting in the mobilization of free water from the myofibrillar lattice and likely causing a higher cooking loss. Thus, corroborating the results obtained in the cooking loss experiment (Fig. 2).

MRI Analysis

MRI is a fast, direct, and non-destructive technique that enables the determination of water distribution in foods as well as the visualization of changes in the internal structures induced by heat treatment (Ezeanaka et al., 2019). Pseudo-colored images enable the user to more readily visualize changes in water mobility and distribution of samples after different heat treatments.

Figure 4a reflects changes in proton density after heat treatment of krill meat. The bright areas in the untreated sample A corresponded to tissues emitting high signal intensities (Bouhrara et al., 2011), indicating that untreated krill meat had the highest water content. With increasing temperatures, the size of bright areas in samples B, C, D, and E gradually decreased, and red-colored areas gradually

changed to blue, indicating a decrease in proton density and an increase in water loss in these krill meat samples. In addition, samples F, G, H, I, and J showed pseudo-colored images when treated at 95 °C for 2, 4, 6, 8, and 10 min, in which red-colored areas decreased with increasing heating time. However, the red-colored areas in samples treated at 95 °C for 8 min were smaller than those treated at 95 °C for 10 min, which is consistent with the cooking loss results. Figures 4b and 4c show the corresponding signal intensities in pseudo-colored images. MRI intensities of samples B, C, D, E, and samples F, G, H, I, and J decreased significantly with increasing temperatures and holding times; MRI signal intensities of samples I and J were consistent with pseudo-colored images (Song et al., 2021). Collectively, these observations confirmed that heat treatment significantly affected water distribution in krill meat.

Microstructure of Heated Krill Meat

Changes in the state of water molecules and water holding capacity are usually related to meat microstructure (Yu et al., 2021). SEM micrographs of microstructural changes in krill meat samples after heat treatment are shown in Fig. 5. The untreated sample A had dense and intact tissue with smooth and flat muscle fiber planes. The microstructure differed significantly after heat treatment compared to untreated samples (Li et al., 2020). The microstructure of samples B, C, D, E, and J changed after heating at different temperatures for 10 min. In contrast, samples B, C, D, E, and J heated for 10 min showed disordered structures and corrugated folded regions, which became increasingly disordered at increasing temperatures. The samples F, G, H, I, and J showed microstructural changes when heated at 95 °C for 2, 4, 6, 8, and 10 min; thus, with prolonged heating times, protein denaturation occurred and muscle tissue contracted, resulting in the formation of corrugated folded structures; treatment for 6 min led to the formation of the densest corrugated folded structures. As holding time extended, corrugated folded structures were destroyed, forming a large area of fractured

(a)

(b)

(c)
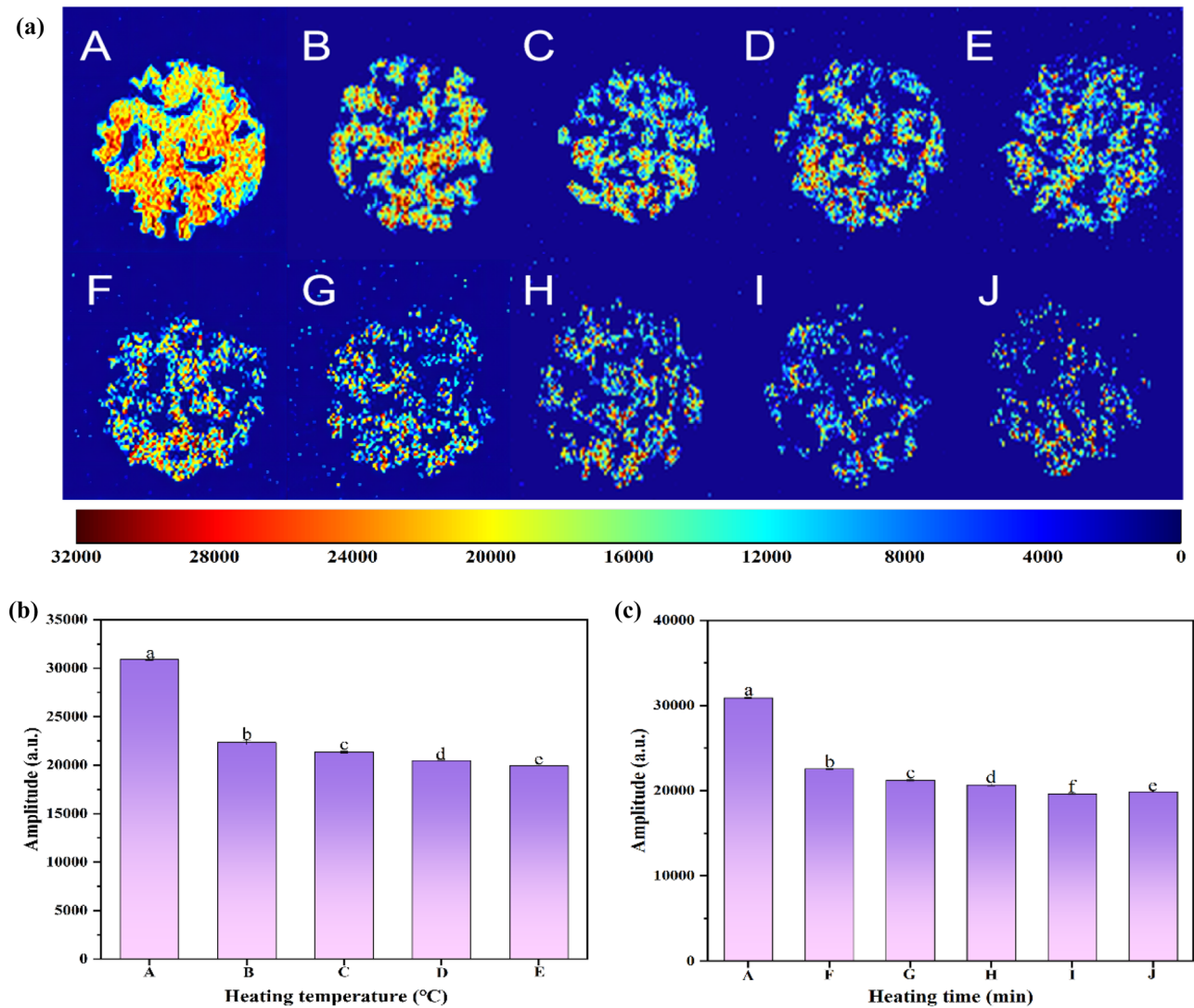
Fig. 4 a Proton density-weighted magnetic resonance of Antarctic krill meat subjected to different heat treatments. **b** Corresponding histograms of signal intensity of the magnetic resonance images (MRI) of samples subjected to different temperatures. **c** Corresponding histograms of signal intensity of the magnetic resonance images (MRI) of heat-treated samples subjected to different holding times. A: untreated; B: 55 °C/10 min; C: 65 °C/10 min; D: 75 °C/10 min; E: 85 °C/10 min; F: 95 °C/2 min; G: 95 °C/4 min; H: 95 °C/6 min; I: 95 °C/8 min; J: 95 °C/10 min. Different letters indicate significant differences between groups ($P < 0.05$)

and disordered structure. (Liu et al., 2019) observed that fibrous bundles in white shrimp subjected to heat treatment were significantly larger and more regular. In contrast, in the present study, the aggregation of corrugated folded structures formed by krill meat and the lower myofibrillar protein content hindered the formation of water-entrapped structures, which might explain the higher water loss rate in Antarctic krill meat than in other shrimp meat.

Intrinsic Fluorescence Analysis

Changes in muscle tissue microstructure are usually associated with changes in the structure of major proteins (Mao et al., 2016). Heat treatment leads to protein denaturation, which alters protein conformation (tertiary structure) mainly due to changes in the location and microenvironment of aromatic amino acid residues. Aromatic amino acid residues can absorb ultraviolet (UV) radiation to fluorescence, and tryptophan (Trp) has a high molar extinction coefficient and is sensitive to the surrounding microenvironment. Thus, changes in the tertiary structure of proteins can be determined by assessing the maximum emission wavelength (λmax) and fluorescence intensity changes in aromatic amino acid residues within the target protein molecule (Shi et al., 2020).

The fluorescence spectra of krill myofibrillar proteins subjected to different temperatures are shown in Fig. 6a.
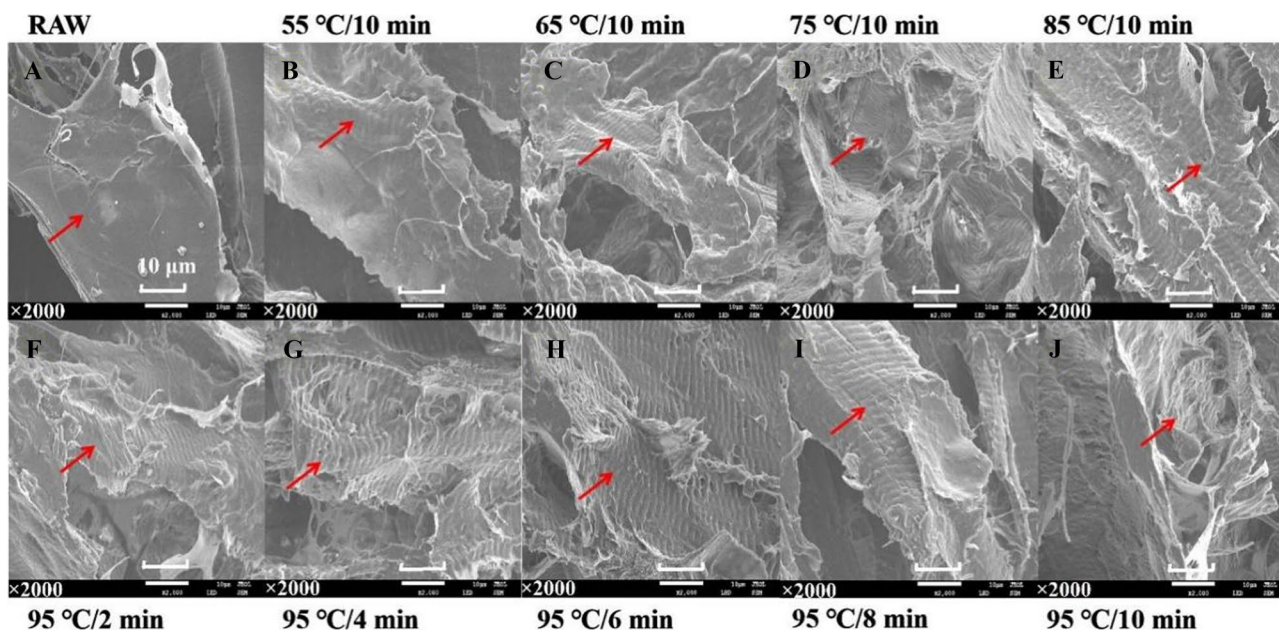
Fig. 5 Scanning electron microscopy (SEM) images of the microstructure of Antarctic krill meat subjected to different heat treatments (magnification 2000×). Scale bar = 10 μm. **A**: untreated; **B**: 55 °C/10 min; **C**: 65 °C/10 min; **D**: 75 °C/10 min; **E**: 85 °C/10 min; **F**: 95 °C/2 min; **G**: 95 °C/4 min; **H**: 95 °C/6 min; **I**: 95 °C/8 min; **J**: 95 °C/10 min

The maximum emission wavelength (λ_{max}) of untreated krill myofibrils (sample A) was 337.5 nm, which is consistent with the findings of (Li et al., 2021b). At increasing temperatures, λ_{max} of myofibrillar proteins in samples A, B, C, D, and E red-shifted from 337.5 nm to 341.5 nm, which could be linked to the gradual exposure of Trp side chains to the aqueous solution, thus increasing the polarity of the surrounding environment. The fluorescence intensity

of Trp residues decreases significantly at temperatures above 55 °C. Considering that heat treatment changed the microstructure of the protein-peptide chain, myofibrillar protein unfolded (Odoli et al., 2019) and Trp residues were exposed on the surface. This enhanced the intermolecular interaction, resulting in the reaggregation of molecules, which further led to more Trp residues being embedded in hydrophobic regions of the protein. This caused a decrease in endogenous
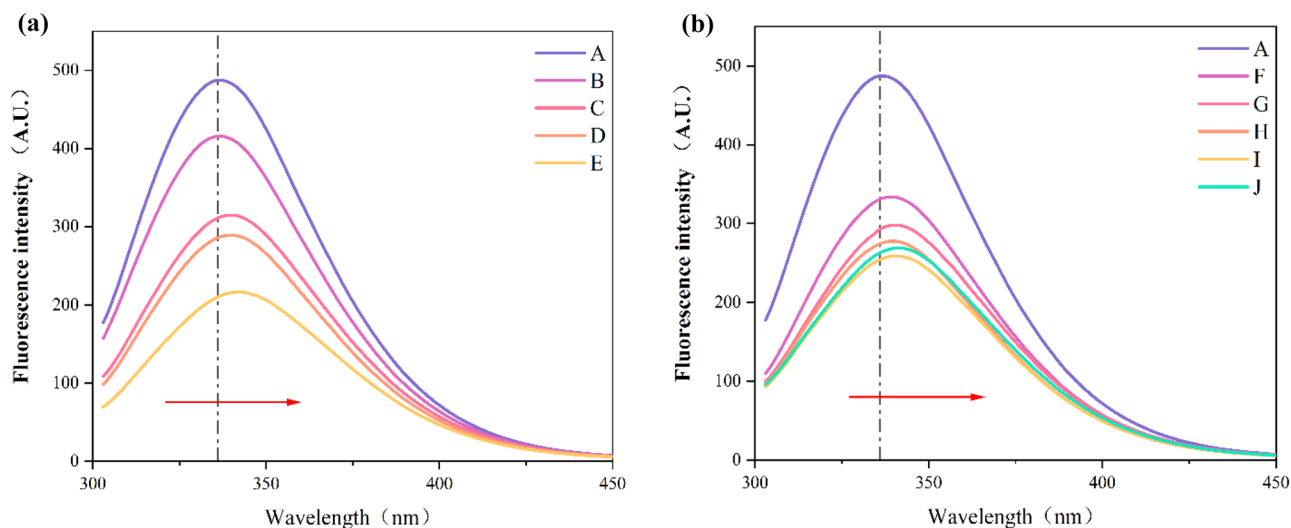
Fig. 6 a Effect of heat treatments at different temperatures on the intrinsic fluorescence of myofibrillar proteins in Antarctic krill meat. **b** Effect of heat treatments at different holding times on the intrinsic fluorescence of myofibrillar proteins in Antarctic krill meat. A: untreated; B: 55 °C/10 min; C: 65 °C/10 min; D: 75 °C/10 min; E: 85 °C/10 min; F: 95 °C/2 min; G: 95 °C/4 min; H: 95 °C/6 min; I: 95 °C/8 min; J: 95 °C/10 min
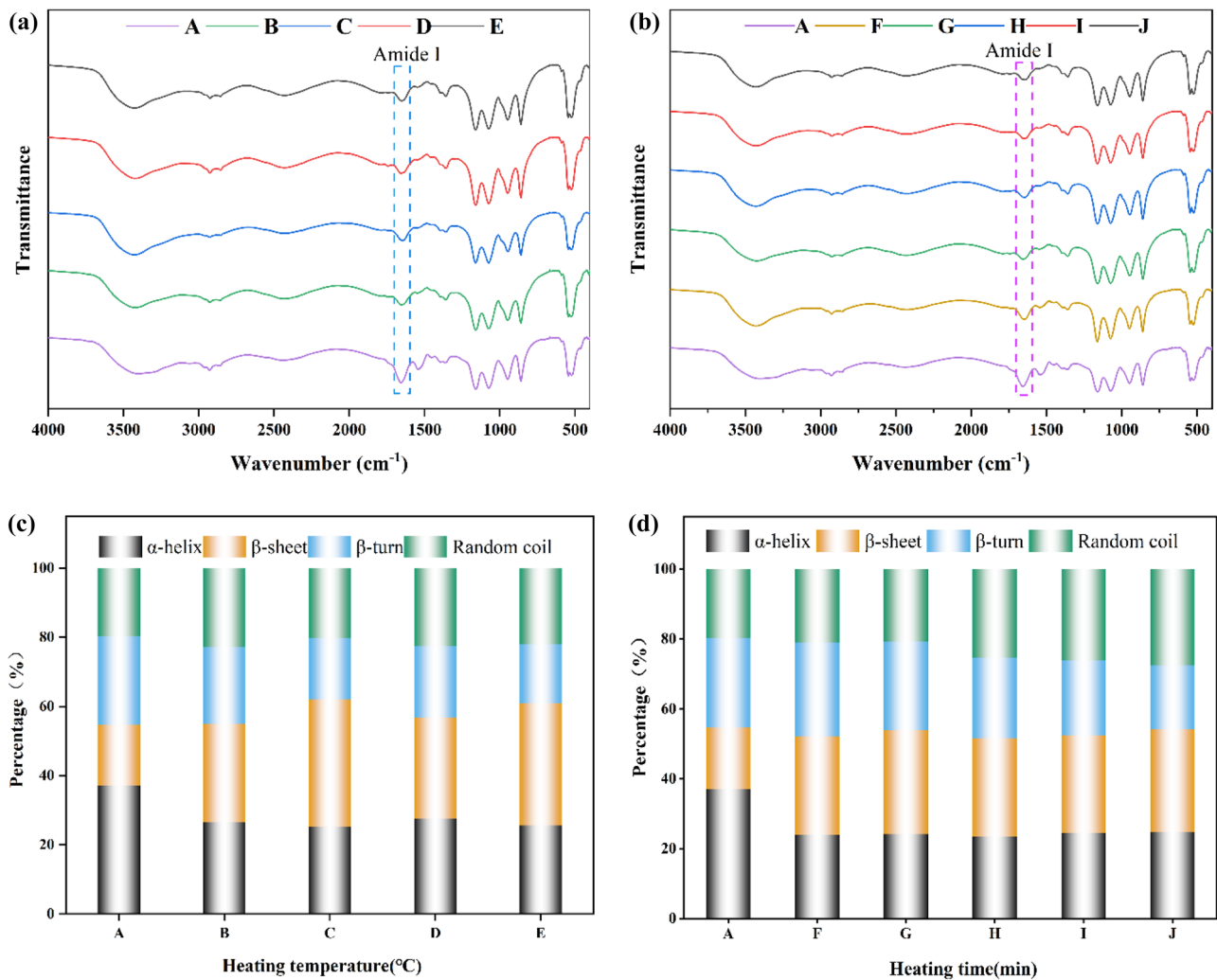
Fig. 7 Effect of heat treatments at different temperatures (**a**) and at different holding times (**b**) on the Fourier transform infrared (FT-IR) spectra of myofibrillar proteins in Antarctic krill meat. Effect of heat treatments at different temperatures (**c**) and at different holding times (**d**) on the content of secondary structure motifs in myofibrillar proteins of Antarctic krill meat. A: untreated; B: 55 °C/10 min; C: 65 °C/10 min; D: 75 °C/10 min; E: 85 °C/10 min; F: 95 °C/2 min; G: 95 °C/4 min; H: 95 °C/6 min; I: 95 °C/8 min; J: 95 °C/10 min

fluorescence intensity (Sun et al., 2013), whereas reaggregation of molecules caused an increase in muscle hardness. As shown in Fig. 6b, samples A, F, G, H, I, and J showed a significant decrease in fluorescence intensity of Trp residues as λ_{max} red-shifted from 337.5 nm to 342.5 nm with extended heating time at 95 °C. The decrease in intrinsic fluorescence intensity and the λ_{max} red shift indicated that the heat treatment caused significant changes in the tertiary structure of myofibrillar protein molecules. However, the fluorescence intensity of samples treated at 95 °C for 8 min was lower than those treated for 10 min, which showed a slight blue shift. This could probably be explained by a transient contraction of the Trp side chain portion induced by heating, followed by a gradual stretching and exposure until the conformation reaches stability, which is consistent with the findings of (Lefèvre et al., 2007).

Changes in Protein Secondary Structure

Changes in the tertiary structure of proteins are determined by changes in secondary structure. FT-IR spectra have been widely used for the characterization of changes in protein structure, mainly focusing on the amide I band (1600–1700 cm^{-1}) (Ovissipour et al., 2017), which was applied to further investigate changes in the structure of krill myofibrillar proteins. Figure 7 shows the percentage of secondary structures in Antarctic krill myofibrillar proteins calculated from amide I in the obtained FT-IR spectra of samples subjected to different heat treatments. Figure 7a, b illustrates that the peak of the amide I band moves to a lower wavenumber as the temperatures increased and holding time extended, indicating a decrease in the degree of molecular order of myofibrillar proteins (Yousefi et al., 2017). The content of α-helix motifs decreased, whereas

Table 3 Effect of heat treatments at different temperatures on the content of secondary structure motifs in the myofibrillar proteins of Antarctic krill meat

Sample	Heat treatment	α-Helix/%	β-Sheet/%	β-Turn/%	Random/%
A	Untreated	35.83 ± 1.90^a	18.24 ± 0.47^c	27.88 ± 1.97^a	18.05 ± 1.81^b
B	55 °C/10 min	26.82 ± 0.69^{bc}	28.06 ± 0.57^b	22.81 ± 0.50^b	22.30 ± 0.52^a
C	65 °C/10 min	24.80 ± 0.55^e	36.32 ± 1.14^a	18.05 ± 1.50^{cd}	20.83 ± 1.05^a
D	75 °C/10 min	28.39 ± 1.36^b	29.00 ± 1.39^b	19.70 ± 1.25^c	22.91 ± 1.11^a
E	85 °C/10 min	25.63 ± 0.99^d	35.72 ± 1.33^a	16.67 ± 1.38^d	21.98 ± 1.65^a

A: untreated sample; B: 55 °C/10 min; C: 65 °C/10 min; D: 75 °C/10 min; E: 85 °C/10 min. Data are presented as means $\pm$ SD (n = 3). Different lowercase letters (a, b, c, d, e) indicate significant differences in the proportion of secondary structure ($P < 0.05$) between treatments at different temperatures

the content of β-sheets increased with increasing temperatures (Fig. 7c and Table 3), indicating that heating-induced protein denaturation, unfolding α-helix deconvolution, and conversion to the β-sheet structure. At lower temperatures, the content of α-helix significantly decreased due to the disruption of hydrogen bonds and hydrophobic bonds of the internal structure of the protein–peptide chain maintaining myofibrillar protein structure (Gao et al., 2021). However, at increasing temperatures, the myofibrillar protein structure underwent more significant changes, muscle structure decomposition, and water loss from inner myofibrils, thus leading to an increase in cooking loss, which is in agreement with the MRI results. Moreover, the increase in the relative content of β-sheets indicated an increase in the number of hydrogen bonds between protein molecules and the degree of aggregation between protein molecules at higher temperatures, leading to a significant increase in hardness. Interestingly, the β-sheet content increased in a non-linear manner, which is in agreement with the findings of (Xu et al., 2010).

In addition, the content of α-helix and β-sheet in samples F, G, H, I, and J did not change significantly (Fig. 7d and Tables 4) with prolonged heating times, probably because after treatment at 95 °C for 2 min, the α-helix structure was completely deconvoluted and transformed into β-sheets, and more β-turn structures were transformed into random coil structures, which increased randomness. Collectively, prolonged heating times increased the randomness of myofibrillar protein structure, and ordered structures gradually changed into an irregular folded structure at higher temperatures (Wijayanti et al., 2014).

SDS-PAGE Analysis

In the present study, changes in protein aggregation, degradation, and solubility in krill myofibrillar proteins were evaluated using SDS-PAGE, and the results are shown in Fig. 8. Myofibrillar proteins in untreated krill meat (lane A) yielded three major protein bands in SDS-PAGE, which corresponded to myosin heavy chain (MHC) (200 kDa), actin (43 kDa), and troponin T (37 kDa) (Jiang et al., 2014). B, C, D, and E lanes corresponded to samples heated at 55, 65, 75, 85 °C for 10 min, while lanes F, G, H, I, and J corresponded to samples heated at 95 °C for 2, 4, 6, 8, and 10 min. With heat treatment, the protein composition of lanes B, C, D, E, and J changed significantly; at temperatures above 75 °C, the MHC band in lanes D and E had reduced intensity and was more degraded in lane J (95 °C/10 min). When heated at 95 °C for 4 min, the degradation of MHC was more pronounced in lanes G, H, I, and J, probably because higher temperatures accelerated protein degradation. Degradation of MHC disrupted the ordered protein structure of krill meat, leading to increased loss of moisture and cooking loss, which is consistent with the results of cooking loss experiments (Fig. 2). After heat treatment, only the bands corresponding to actin and troponin could be observed in lanes D, E, G, H, I, and J. These results indicated that the thermostability of actin is significantly higher compared to myosin (Qi et al., 2018). Moreover, troponin band intensity in lanes B, C, D, and E and lanes F, G, H, I, and J were only slightly decreased, which suggests that troponin is also heat stable, as suggested by (Hu et al., 2017).

Table 4 Effect of heat treatments at different holding times on the content of secondary structure motifs in the myofibrillar proteins of Antarctic krill meat

Sample	Heat treatment	α-Helix/%	β-Sheet/%	β-Turn/%	Random/%
A	Untreated	35.83 ± 1.90^a	18.24 ± 0.47^a	27.88 ± 1.97^a	18.05 ± 1.81^c
F	95 °C/2 min	24.81 ± 0.79^b	27.96 ± 0.17^b	26.81 ± 1.02^a	20.42 ± 0.77^b
G	95 °C/4 min	24.09 ± 0.57^{bc}	28.23 ± 1.44^b	27.20 ± 1.73^a	20.49 ± 0.56^b
H	95 °C/6 min	22.52 ± 0.83^c	28.01 ± 0.47^b	23.77 ± 0.52^b	25.70 ± 0.43^a
I	95 °C/8 min	24.93 ± 0.66^b	28.17 ± 0.43^b	20.92 ± 0.78^c	25.98 ± 0.38^a
J	95 °C/10 min	24.71 ± 0.39^b	29.15 ± 0.54^b	18.92 ± 0.65^c	27.21 ± 0.40^a

A: untreated; G: 95 °C/4 min; F: 95 °C/2 min; H: 95 °C/6 min; I: 95 °C/8 min; J: 95 °C/10 min. Data are presented as means $\pm$ SD (n = 3). Different lowercase letters (a, b, c, d, e) indicate significant differences in the proportion of secondary structure ($P < 0.05$) between treatments at different holding times
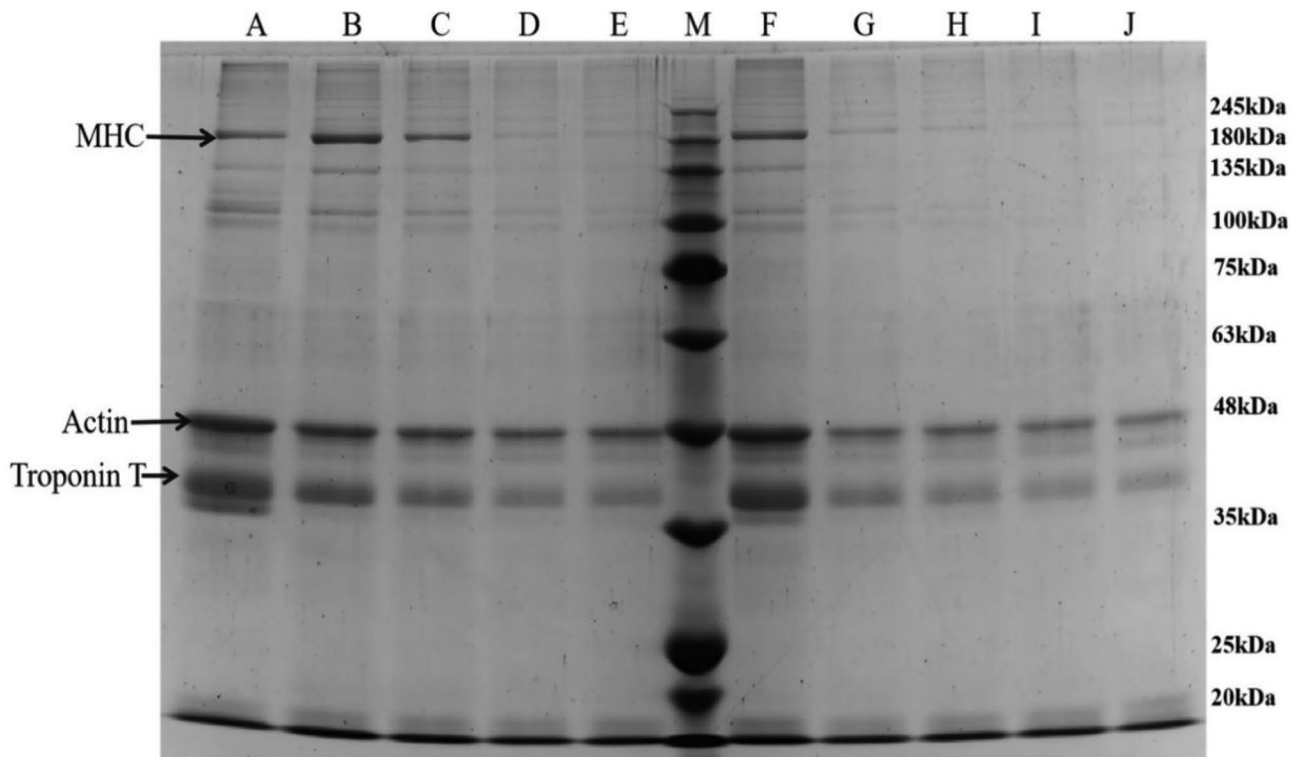
Fig. 8 SDS-PAGE profiles of Antarctic krill myofibrillar proteins subjected to different heat treatments. M: molecular weight standard. **A**: untreated; **B**: 55 °C/10 min; **C**: 65 °C/10 min; **D**: 75 °C/10 min; **E**: 85 °C/10 min; **F**: 95 °C/2 min; **G**: 95 °C/4 min; **H**: 95 °C/6 min; **I**: 95 °C/8 min; **J**: 95 °C/10 min

Due to changes in the dynamic balance of acid-based groups on the surface of proteins caused by the degradation of myofibrillar protein, the formation of disulfide bonds between denatured myofibrillar protein may further promote cross-linking between protein molecules (Ko et al., 2007), resulting in increased muscle contraction, water loss, and hardness.

Conclusion

This study aimed to elucidate the effects of heat treatment based on different temperatures and holding times on the quality attributes of Antarctic krill meat. Heat-treated krill meat had increased hardness and chewiness, with severe cooking loss and leakage of immobilized water. This can be mainly due to denaturation and degradation of myofibrillar proteins induced by heating. In fact, the content of α-helix structures was reduced in heat-treated samples, indicating the transformation of α-helix motifs into β-sheet structures, which resulted in changes in the hydrophobic regions of myofibrillar proteins and were reflected in the protein microstructure. In particular, myofibrillar proteins denatured and aggregated after heating and showed increased muscle contraction, thus forming corrugated aggregates, which did not yield a water-entrapped structure, thus resulting in a significant water loss. These findings may support the observations of increased hardness and loss of quality in krill meat after heat treatment.

Declarations

Conflict of Interest The authors declare no competing interests.

References

Atkinson, A., Siegel, V., Pakhomov, E. A., Jessopp, M. J., & Loeb, V. (2009). A re-appraisal of the total biomass and annual production of Antarctic krill. *Deep Sea Research Part i: Oceanographic Research Papers, 56*(5), 727–740.

Bi, S., Huang, Z., Wang, Y., Nie, F., Wang, X., Sun, L., Zhu, Z., & Gooneratne, R. (2019). Effects of T-2 toxin on histopathology, fatty acid and water distribution of shrimp (Litopenaeus vannamei) muscle. *Journal of Environmental Science and Health, Part B, 54*, 1–8.

Bouhrara, M., Clerjon, S., Damez, J.-L., Chevarin, C., Portanguen, S., Kondjoyan, A., & Bonny, J.-M. (2011). Dynamic MRI and Thermal Simulation To Interpret Deformation and Water Transfer in Meat during Heating. *Journal of Agricultural and Food Chemistry, 59*, 1229–1235.

Cavan, E., Belcher, A., Atkinson, A., Hill, S., Kawaguchi, S., McCormack, S., Meyer, B., Nicol, S., Ratnarajah, L., Schmidt, K., Steinberg, D., Tarling, G., & Boyd, P. (2019). The importance of Antarctic krill in biogeochemical cycles. *Nature Communications, 10*, 4742.

Chen, L., Bao, P., Wang, Y., Hu, Y., Fang, H., Yang, H., Zhang, B., He, B., & Zhou, C. (2022). Improving quality attributes of refrigerated prepared pork chops by injecting l-arginine and l-lysine solution. *LWT - Food Science and Technology, 153*, 112423.

Chen, L., Zhang, G.-H., & Zhang, W.-G. (2015). Effects of High Oxygen Packaging on Tenderness and Water Holding Capacity of Pork Through Protein Oxidation. *Food and Bioprocess Technology, 8*(11), 2287–2297.

Chen, Y., Xu, A., Yang, R., Jia, R., Zhang, J., Xu, D., & Yang, W. (2020). Myofibrillar Protein Structure and Gel Properties of Trichiurus Haumela Surimi Subjected to High Pressure or High Pressure Synergistic Heat. *Food and Bioprocess Technology, 13*, 589–598.

Chen, Y. C., & Jaczynski, J. (2007). Gelation of protein recovered from whole Antarctic krill (Euphausia superba) by isoelectric solubilization/precipitation as affected by functional additives. *Journal of Agricultural and Food Chemistry, 55*(5), 1814–1822.

Ellingsen, T. E., & Mohr, V. (1987). Biochemistry of the autolytic processes in Antarctic krill post mortem Autoproteolysis. *Biochemical Journal, 246*(2), 295–305.

Ezeanaka, M., Nsor-Atindana, J., & Zhang, M. (2019). Online Low-field Nuclear Magnetic Resonance (LF-NMR) and Magnetic Resonance Imaging (MRI) for Food Quality Optimization in Food Processing. *Food and Bioprocess Technology, 12,* 1435–1451.

Gao, X., Guo, W., Wu, N., Yao, Y., Du, H., Xu, M., Zhao, Y., & Tu, Y. (2021). Effects of salt and heat treatment on the physicochemical properties, microstructure, secondary structure and simulated in vitro gastrointestinal digestion of duck egg white. *Journal of the Science of Food and Agriculture, 101*, 6093–6103.

Haghighi, H., Belmonte, A. M., Masino, F., Minelli, G., Lo Fiego, D., & Pulvirenti, A. (2021). Effect of Time and Temperature on Physicochemical and Microbiological Properties of Sous Vide Chicken Breast Fillets. *Applied Sciences, 111*, 3189.

Hassoun, A., Aït-Kaddour, A., Sahar, A., & Cozzolino, D. (2021). Monitoring Thermal Treatments Applied to Meat Using Traditional Methods and Spectroscopic Techniques: A Review of Advances over the Last Decade. *Food and Bioprocess Technology, 14*(2), 195–208.

Hu, L., Ren, S., Shen, Q., Chen, J., Ye, X., & Ling, J. (2017). Proteomic study of the effect of different cooking methods on protein oxidation in fish fillets. *RSC Advances, 7*, 27496–27505.

Huang, Y., Guo, L., Xiong, S., & Li, A. (2016). Property and structure changes of myofibril protein in pork treated by high pressure combined with heat. *Food Science and Technology International, 22*(7), 647–662.

Ishamri, I., Hwang, Y.-H., & Joo, S.-T. (2019). Effect of Different Temperature and Time Combinations on Quality Characteristics of Sous-vide Cooked Goat Gluteus Medius and Biceps Femoris. *Food and Bioprocess Technology, 12*, 1000–1009.

Jiang, Q., Han, J., Gao, P., Yu, L., Xu, Y., & Xia, W. (2018). Effect of heating temperature and duration on the texture and protein composition of Bighead Carp (Aristichthys nobilis) muscle. *International Journal of Food Properties, 21*, 2110–2120.

Jiang, Q., Li, S., Xu, Y., & Xia, W. (2014). Nutrient Compositions and Properties of Antarctic Krill (Euphausia superba) Muscle and Processing By-Products. *Journal of Aquatic Food Product Technology, 25*, 434–443.

Ko, W.-C., Yu, C.-C., & Hsu, K.-C. (2007). Changes in conformation and sulfhydryl groups of tilapia actomyosin by thermal treatment. *LWT - Food Science and Technology, 40*, 1316–1320.

Lee, Y.-C., Lin, C.-Y., Wei, C.-I., Tung, H.-N., Chiu, K., & Tsai, Y.-H. (2021). Preliminary Evaluation of a Novel Microwave-Assisted Induction Heating (MAIH) System on White Shrimp Cooking. *Foods, 10*, 545.

Lefèvre, F., Fauconneau, B., Thompson, J., & Gill, T. (2007). Thermal Denaturation and Aggregation Properties of Atlantic Salmon Myofibrils and Myosin from White and Red Muscles. *Journal of Agricultural and Food Chemistry, 55*, 4761–4770.

Li, X., Llave, Y., Fukuoka, M., & Sakai, N. (2020). Physicochemical changes in cooked prawn muscle with or without shell during water bath treatment: Effect of thermal protein denaturation. *Journal of Food Process Engineering, 43*(10), e13505.

Li, X., Llave, Y., Mao, W., Fukuoka, M., & Sakai, N. (2018). Heat and mass transfer, shrinkage, and thermal protein denaturation of kuruma prawn (Marsupenaeus japonicas) during water bath treatment: A computational study with experimental validation. *Journal of Food Engineering, 238*, 30–43.

Li, Y., Zeng, Q.-H., Liu, G., Peng, Z., Wang, Y., Zhu, Y., Liu, H., Zhao, Y., & Jing Wang, J. (2021a). Effects of ultrasound-assisted basic electrolyzed water (BEW) extraction on structural and functional properties of Antarctic krill (Euphausia superba) proteins. *Ultrasonics Sonochemistry, 71*, 105364.

Li, Y., Zeng, Q. H., Liu, G., Peng, Z., Wang, Y., Zhu, Y., Liu, H., Zhao, Y., & Jing Wang, J. (2021b). Effects of ultrasound-assisted basic electrolyzed water (BEW) extraction on structural and functional properties of Antarctic krill (Euphausia superba) proteins. *Ultrasonics Sonochemistry, 71*, 105364.

Lin, J., Zhang, Y., Li, Y., Sun, P., Ren, X., & Li, D. (2021). Improving the texture properties and protein thermal stability of Antarctic krill (Euphausia superba) by L-lysine marination. *Journal of the Science of Food and Agriculture.* https://doi.org/10.1002/jsfa.11741

Ling, B., Tang, J., Kong, F., Mitcham, E. J., & Wang, S. (2015). Kinetics of Food Quality Changes During Thermal Processing: A Review. *Food and Bioprocess Technology, 8*(2), 343–358.

Ling, J.-G., Xuan, X.-T., Yu, N., Cui, Y., Shang, H.-T., Liao, X.-J., Lin, X.-D., Yu, J.-F., & Liu, D.-H. (2020). High pressure-assisted vacuum-freeze drying: A novel, efficient way to accelerate moisture migration in shrimp processing: Moisture migration in HPP-VFD shrimp. *Journal of Food Science, 85*(4), 1167–1176.

Liu, L., Liu, C., & Li, J. (2011). Comparison of Biochemical Composition and Nutritional Value of Antarctic Krill (Euphausia Superb) with Several Species of Shrimps. *Advanced Materials Research, 361–363*, 799–803.

Liu, M., Liu, S.-H., Han, T.-J., Xia, F., Li, M.-S., Weng, W., Chen, G.-X., Cao, M.-J., & Liu, G. (2019). Effects of thermal processing on digestion stability and immunoreactivity of the Litopenaeus vannamei matrix. *Food & Function, 10*, 5374–5385.

Mao, W., Li, X., Fukuoka, M., Liu, S., Ji, H., & Sakai, N. (2016). Study of Ca2+-ATPase Activity and Solubility in the Whole Kuruma Prawn (Marsupenaeus japonicus) Meat During Heating: Based on the Kinetics Analysis of Myofibril Protein Thermal Denaturation. *Food and Bioprocess Technology, 9*(9), 1511–1520.

Niamnuy, C., Devahastin, S., & Soponronnarit, S. (2008). Changes in protein compositions and their effects on physical changes of shrimp during boiling in salt solution. *Food Chemistry, 108*(1), 165–175.

Odoli, C. O., Oduor-Odote, P., & Arason, S. (2019). The influence of lipid content and pretreatment methods on protein conformation in fish (capelin, Mallotus villosus) during smoking and drying. *Food Science and Nutrition, 7*(4), 1446–1454.

Ovissipour, R., Rasco, B., Tang, J., & Sablani, S. (2017). Kinetics of Protein Degradation and Physical Changes in Thermally Processed Atlantic Salmon (Salmo salar). *Food and Bioprocess Technology, 10*, 1865–1882.

Peng, Y., Ji, W., Zhang, D., Ji, H., & Liu, S. (2019). Composition and content analysis of fluoride in inorganic salts of the integument of Antarctic krill (Euphausia superba). *Scientific Reports, 9*, 7853.

Purslow, P. P., Oiseth, S., Hughes, J., & Warner, R. D. (2016). The structural basis of cooking loss in beef: Variations with temperature and ageing. *Food Research International, 89*, 739–748.

Qi, J., Li, X., Zhang, W., Wang, H., Zhou, G., & Xu, X. (2018). Influence of stewing time on the texture, ultrastructure and in vitro digestibility of meat from the yellow-feathered chicken breed. *Animal Science Journal, 89*(2), 474–482.

Shi, H., Zhang, X., Chen, X., Fang, R., Zou, Y., Wang, D., & Xu, W. (2020). How ultrasound combined with potassium alginate marination tenderizes old chicken breast meat: Possible mechanisms from tissue to protein. *Food Chemistry, 328*, 127144.

Song, Y., Huang, F., Li, X., Han, D., Zhao, L., Liang, H., Rui, M., Wang, J., & Zhang, C. (2021). Water status evolution of pork blocks at different cooking procedures: A Two-dimensional LF-NMR T1–T2 relaxation study. *Food Research International, 148*, 110614.

Straadt, I. K., Rasmussen, M., Andersen, H. J., & Bertram, H. C. (2007). Aging-induced changes in microstructure and water distribution in fresh and cooked pork in relation to water-holding capacity and cooking loss – A combined confocal laser scanning microscopy (CLSM) and low-field nuclear magnetic resonance relaxation study. *Meat Science, 75*(4), 687–695.

Strzelczak, A., Balejko, J., Szymczak, M., & Witczak, A. (2021). Effect of Protein Denaturation Temperature on Rheological Properties of Baltic Herring (Clupea harengus membras) Muscle Tissue. *Foods, 10*, 829.

Sun, S., Wang, S., Lin, R., Cheng, S., Yuan, B., Wang, Z., & Tan, M. (2020). Effect of Different Cooking Methods on Proton Dynamics and Physicochemical Attributes in Spanish Mackerel Assessed by Low-Field NMR. *Foods, 9*(3), 364.

Sun, W., Zhou, F., Sun, D.-W., & Zhao, M. (2013). Effect of Oxidation on the Emulsifying Properties of Myofibrillar Proteins. *Food and Bioprocess Technology, 6*(7), 1703–1712.

Szczesniak, A. S. (2002). Texture is a sensory property. *Food Quality and Preference, 13*(4), 215–225.

Urango, A. C. M., Strieder, M. M., Silva, E. K., & Meireles, M. A. A. (2022). Impact of Thermosonication Processing on Food Quality and Safety: A Review. *Food and Bioprocess Technology*. https://doi.org/10.1007/s11947-022-02760-0

Wang, H., Luo, Y., & Shen, H. (2013). Effect of frozen storage on thermal stability of sarcoplasmic protein and myofibrillar protein from common carp (Cyprinus carpio) muscle. *International Journal of Food Science & Technology, 48*(9), 1962–1969.

Wang, K., Lin, X., Zhao, W., Fan, X., Yu, W., Ma, Z., Yu, C., & Dong, X. (2020). Low-temperature steaming improves eating quality of whitefish. *Journal of Texture Studies, 51*(5), 830–840.

Wang, L.-Z., Xue, C.-H., Xue, Y., Wang, Y.-M., & Li, J.-Z. (2015). Optimization and evaluation of a novel technique for hydrolyzing Antarctic krill (Euphausia superba) proteins. *Food and Bioproducts Processing, 94,* 629–636.

Wijayanti, H. B., Bansal, N., & Deeth, H. C. (2014). Stability of Whey Proteins during Thermal Processing: A Review. *Comprehensive Reviews in Food Science and Food Safety, 13*(6), 1235–1251.

Xia, K., Xu, W., Huang, L., Song, Y., Zhu, B.-W., & Tan, M. (2018). Water dynamics of turbot flesh during frying, boiling, and stewing processes and its relationship with color and texture properties: Low-field NMR and MRI studies. *Journal of Food Processing and Preservation, 42*(1), e13338.

Xu, D., Yang, X., Wang, Y., & Sun, L. (2020). Cascading Mechanism Triggering the Activation of Polyphenol Oxidase Zymogen in Shrimp Litopenaeus vannamei After Postmortem and the Correlation with Melanosis Development. *Food and Bioprocess Technology, 13*(7), 1131–1145.

Xu, X.-L., Han, M., Fei, Y., & Zhou, G. H. (2010). Raman spectroscopic study of heat-induced gelation of pork myofibrillar proteins and its relationship with textural characteristic. *Meat Science, 87*, 159–164.

Yang, F., Jia, S., Liu, J., Gao, P., Yu, D., Jiang, Q., Xu, Y., Yu, P., Xia, W., & Zhan, X. (2019). The relationship between degradation of myofibrillar structural proteins and texture of superchilled grass carp (Ctenopharyngodon idella) fillet. *Food Chemistry, 301*, 125278.

Yousefi, M., Ariffin, F., & Huda, N. (2017). An alternative source of type I collagen based on by-product with higher thermal stability. *Food Hydrocolloids, 63*, 372–382.

Yu, M.-M., Li, D.-Y., Liu, Z.-Q., Liu, Y.-X., Zhou, J.-Z., Zhang, M., Zhou, D.-Y., & Zhu, B.-W. (2021). Effects of heat treatments on texture of abalone muscles and its mechanism. *Food Bioscience, 44*, 101402.

Zhang, F., Jiang, S., Feng, X., Wang, R., Zeng, M., & Zhao, Y. (2020). Physicochemical state and in vitro digestibility of heat treated water-soluble protein from Pacific oyster (Crassostrea gigas). *Food Bioscience, 34*, 100528.

Zhang, L., Zhang, F., & Wang, X. (2016). Changes of protein secondary structures of pollock surimi gels under high-temperature (100 °C and 120 °C) treatment. *Journal of Food Engineering, 171*, 159–163.

Zheng, Y. Y., Zhou, C., Wang, C., Ding, D. M., Wang, J. J., Li, C. B., & Zhou, G. H. (2020). Evaluating the effect of cooking temperature and time on collagen characteristics and the texture of hog maw. *Journal of Texture Studies, 52*(2), 207–218.

Zhu, Z., Zhao, Y., Zhang, Y., Wu, X., Liu, J., Shi, Q., & Fang, Z. (2021). Effects of ultrasound pretreatment on the drying kinetics, water status and distribution in scallop adductors during heat pump drying. *Journal of the Science of Food and Agriculture, 101*(15), 6239–6247.